JB Review
Rotation and structure of F_oF_1-ATP synthase

Daichi Okuno, Ryota Iino and Hiroyuki Noji*

Department of Applied Chemistry, School of Engineering, The University of Tokyo, Bunkyo-ku, Tokyo 113-8656, Japan

*Hiroyuki Noji, Department of Applied Chemistry, School of Engineering, The University of Tokyo, Bunkyo-ku, Tokyo 113-8656, Japan. Tel: +81-3-5841-7252, Fax: +81-3-5841-1872, email: hnoji@appchem.t.u-tokyo.ac.jp

F_oF_1-ATP synthase is one of the most ubiquitous enzymes; it is found widely in the biological world, including the plasma membrane of bacteria, inner membrane of mitochondria and thylakoid membrane of chloroplasts. However, this enzyme has a unique mechanism of action: it is composed of two mechanical rotary motors, each driven by ATP hydrolysis or proton flux down the membrane potential of protons. The two molecular motors interconvert the chemical energy of ATP hydrolysis and proton electrochemical potential *via* the mechanical rotation of the rotary shaft. This unique energy transmission mechanism is not found in other biological systems. Although there are other similar man-made systems like hydroelectric generators, F_oF_1-ATP synthase operates on the nanometre scale and works with extremely high efficiency. Therefore, this enzyme has attracted significant attention in a wide variety of fields from bioenergetics and biophysics to chemistry, physics and nanoscience. This review summarizes the latest findings about the two motors of F_oF_1-ATP synthase as well as a brief historical background.
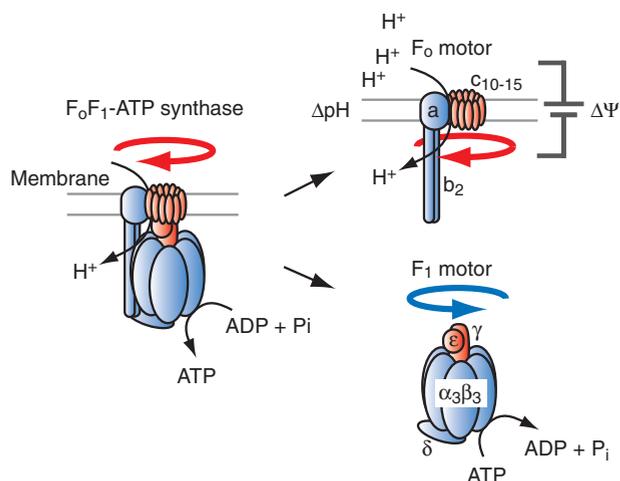
F_oF_1-ATP synthase

Adenosine-5′-triphosphate (ATP) is the ubiquitous energy currency of the cell. The human body contains about 50 g of ATP that is sustained by strict dynamic equilibrium between hydrolysis and synthesis. The total ATP produced under basal metabolism in humans amounts to 50–75 kg per day, and the same amount of ATP is consumed for the large variety of energy-requiring reactions such as muscle contraction, synthesis of biomolecules and mass transfer across biomembranes. Under aerobic conditions, the major ATP synthesis pathway is oxidative phosphorylation of which the terminal reaction is catalysed by F_oF_1-ATP synthase.

This enzyme is found widely in the biological world, including in thylakoid membranes, the mitochondrial inner membrane and the plasma membrane of bacteria. This enzyme catalyses ATP synthesis from adenosine diphosphate (ADP) and inorganic phosphate (P_i) by using the electrochemical potential of protons (or sodium ions in some bacteria) across the membrane, i.e. it converts the electrochemical potential into its chemical form. This enzyme also functions in the reverse direction when the electrochemical potential becomes insufficient: it catalyses proton pumping to form an electrochemical potential to hydrolyse ATP into ADP and P_i. F_oF_1-ATP synthase is a supercomplex enzyme with a molecular weight of >500 kDa and consists of two rotary motors. One is F_1 (~380 kDa), which is the water-soluble part of ATP synthase. When isolated from the membrane portion, it acts as an ATP-driven motor: it rotates its inner subunit to hydrolyse ATP and is therefore termed F_1-ATPase. The other rotary motor of ATP synthase is F_o (~120 kDa), which is embedded in the membrane and generates rotary torque upon proton translocation that is driven by proton electrochemical potential (Fig. 1) (*1*). Bacterial F_1 is composed of $\alpha_3\beta_3\gamma\delta\epsilon$-subunits. The three α- and β-subunits form the hexameric stator ring in which the α- and β-subunits are alternately arranged. The rotor shaft is the γ-subunit, which is accommodated in the central cavity of the $\alpha_3\beta_3$-ring. The ε-subunit binds onto the protruding part of the γ-subunit and provides a connection between the rotor parts of F_1 and F_o. The ε-subunit acts as the endogenous inhibitor of F_1 (*2–4*), by transforming the conformational state from the closed form to extended form that blocks the γ rotation due to steric hindrance (*5–8*). This inhibitory function is thought to be physiologically important to avoid ATP consumption (*9*). The δ-subunit acts as a connector between F_1 and F_o that connects the stator parts. Thus, the minimum complex of F_1 as a motor is the $\alpha_3\beta_3\gamma$ subcomplex. Catalytic reaction centres for ATP hydrolysis/synthesis reside at the three α—β interfaces, which are on the anticlockwise side of the β-subunit as indicated with red circles in Fig. 2A. The non-catalytic ATP-binding sites reside on the other α/β interfaces. While the catalytic site is formed mainly with amino-acid residues from the β-subunit, the non-catalytic sites are primarily within the α-subunit. Upon ATP hydrolysis on the catalytic sites, F_1 rotates the γ-subunit in the anticlockwise direction viewed from the F_o side. F_o part consists of ab_2c_{10-15} subunits. The number of *c* subunits varies among species. For example, the copy number of the *c* subunit is eight in bovine mitochondria (*10*), 10 in yeast (*11*), *Escherichia coli* (*12*) and thermophilic *Bacillus* PS3 (*13*), 11 in *Ilyobacter tartaricus* (*14, 15*),
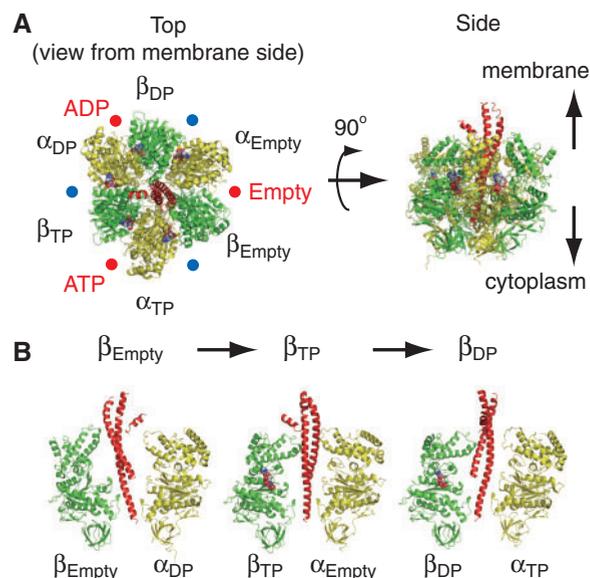
Featured Article

Fig. 1 F_o and F_1 motors of ATP synthase. Schematic images of F_oF_1-ATP synthase. The rotor and stator parts are shown in red and blue, respectively. The subunit composition of bacterial F_o is ab_2c_{10-15} (the number of c subunits varies from 10 to 15 in different species). F_o is embedded in the cell membrane and rotates the c-ring against the ab_2 stator, driven by passive proton translocation along the proton electrochemical potential that comprises the proton concentration (ΔpH) and membrane voltage ($\Delta\Psi$) across the membrane. Bacterial F_1 is composed of $\alpha_3\beta_3\gamma\delta\varepsilon$ and is an ATP-driven rotary motor in which the γ-subunit rotates against the $\alpha_3\beta_3$-cylinder. The ε-subunit binds to the protruding part of the γ-subunit. The δ binds to the bottom of the $\alpha_3\beta_3$-ring (note that the rotational direction of F_o is opposite to that of F_1). In the whole complex of F_oF_1, F_o reverses the rotation of F_1, leading to ATP synthesis from ADP and P_i.

Fig. 2 Crystal structure of the $\alpha_3\beta_3\gamma$ subcomplex of F_1. The crystal structure of F_1 from bovine mitochondria (PDB code; 1BMF). The α-, β- and γ-subunits are shown in yellow, green and red, respectively. (A) The left figure is viewed from the membrane side (F_o side), and is rotated 90° in anticlockwise direction to arrow (right figure). The protruding part of γ is directed toward the membrane side (15). The catalytic sites are located at the α–β interface indicated by red circles, which are primarily on the β-subunit. Each site carries AMP-PNP, ADP, or is empty and is designated as β_{TP}, β_{DP}, or β_{Empty}, respectively. The other interfaces are non-catalytic sites (blue circles), all of which bind with AMP-PNP. Each α-subunit forming a catalytic site with the β-subunit is designated as α_{TP}, α_{DP} and α_{Empty}, respectively. (B) Conformational states of the β-subunit and the catalytic α–β interfaces. Three α–β pairs with the γ-subunit are shown in yellow and green with the central γ-subunit (red). The α and β-subunits are composed of the N-terminal domain, nucleotide-binding domain and C-terminal domain (from bottom to top). β_{Empty} has an open conformation in which the α-helical C-terminal domain rotates upwards to open the cleft of the nucleotide-binding pocket. Both β_{ATP} and β_{ADP} have a closed conformation entrapping the nucleotide within the closed pocket.

Propionigenium modestum (16) and *Clostridium paradpxum* (17), 13 in thermoalkaliphilic *Bacillus* TA2.TA1 (18) and *Bacillus pseudofirmus* OF4 (19), 14 in spinach chloroplast (20) and 15 in *Spirulina platensis* (21). The c subunits form a ring complex by aligning in a circle. It is widely thought that the c-ring and the a subunit form a proton pathway (for details, see the 'Proton translocation pathway of F_o' section). With the downhill proton flow through the proton channel, the c-ring rotates against the ab_2 subunits in the opposite direction of the γ-subunit of the F_1 motor (22). Thus, in the F_oF_1 complex, F_o and F_1 push each other in the opposite direction. Under physiological condition where the electrochemical potential of the protons is large enough to surpass the free energy of ATP hydrolysis, F_o forcibly rotates the γ-subunit in the clockwise direction and then F_1 catalyses the reverse reaction, i.e. ATP synthesis which is the principle physiological function of ATP synthase. In contrast, when the electrochemical potential is small or decreases, F_1 forces F_o to rotate the c-ring in the reverse direction to pump protons against the electrochemical potential.

Binding change mechanism and structure of F_1-ATPase

The three catalytic sites on the β-subunits work co-operatively during catalysis. The classic working model for F_1 is the 'binding-change mechanism' proposed by Paul Boyer (23). The early stage of this model

postulated alternating transition between two chemical states, assuming two catalytic sites residing on F_1. It was later revised to propose the cyclic transition of the catalytic states among three catalytic sites based on the biochemical and electron microscopic experiments that revealed that F_1 has the three catalytic sites (24–26). One important feature of this model is that the affinity for nucleotide at each catalytic site is different from each other at any given time, and the status of the three β-subunits cooperatively change in one direction accompanying γ rotation. This hypothesis is strongly supported by X-ray crystallographic studies performed by Walker's group (27). The first resolved crystal structure of F_1 (27) revealed many essential structural features of F_1 at atomic resolution. Importantly, the catalytic β-subunits differ from each other in conformation and catalytic state: one binds to an ATP analogue, adenosine-5′-(β,γ-imino)-triphosphate (AMP-PNP), the second binds to ADP and the third site is empty (Fig. 2A). Therefore, these sites are termed β_{TP}, β_{DP} and β_{Empty}, respectively. While β_{TP} and β_{DP} have a closed conformation wrapping bound nucleotides on the catalytic sites, β_{Empty} has an open conformation

swinging the C-terminal domain away from the binding site to open the cleft of the catalytic site (Fig. 2B). These features are consistent with the binding-change mechanism. Another important feature found in the crystal structure is that while the N-terminal domains of the α and β-subunits form a symmetrical smooth cavity as the bearing for γ rotation at the bottom of the $α_3β_3$-ring, the C-terminal domains of the β-subunit show distinct asymmetric interactions with the γ-subunit. Therefore, the most feasible inference is that the open-to-closed transition of the β-subunits upon ATP binding pushes γ, and the sequential conformational change among β-subunits leads the unidirectional γ rotation, which was recently visualized in simultaneous imaging of the conformational change of the β-subunit and the γ rotation (28).

Verification of F_1 rotation by single-molecule observation

Since the publication of the crystal structure, many studies have attempted to demonstrate the rotation of F_1. Crosslink exchange experiment between the β- and γ-subunits of F_1 derived from *E. coli* (29) and the polarized absorption relaxation of F_1 from spinach chloroplasts (30) have proven the rotational motion of the γ-subunit during catalysis. Unidirectional rotation of the γ-subunit upon ATP hydrolysis was proved with the direct observation of F_1 rotation from thermophilic *Bacillus* PS3 (TF_1) under the microscope (31). In order to suppress rotary Brownian motion study, F_1 was immobilized on a glass surface modified with Ni-nitrilotriacetic acid (NTA) thorough the interaction between Ni^{2+} and the His-tag, which was introduced into the N-terminus of the β-subunit. In addition, a fluorescently labelled actin filament with length of 0.6–4 μm and diameter of 10 nm was attached to the γ-subunit as the rotation marker to magnify the subtle motion of the γ-subunit of which the radius is only 1 nm, which is much smaller than the spatial resolution (∼200 nm) of a conventional microscope (Fig. 3A). Note that in recent studies, other types of probes such as polystyrene beads, gold colloidal beads, gold nanorods, and magnetic beads are frequently used instead of actin filaments because the imaging of fluorescently labelled actin filaments suffers from photobleaching. The rotational direction is always anticlockwise when viewed from the F_o side and, importantly, it was consistent with the expected rotary direction from the crystal structure. Assuming the β-subunit undergoes the conformational transition from $β_{Empty}$, $β_{TP}$ and $β_{DP}$, each catalytic state propagates in the anticlockwise direction, accompanying the anticlockwise γ rotation. The rotational velocity was far slower than the expected rate from bulk ATPase measurements because of the large hydrodynamic friction exerted on the rotating actin filament. However, this allows us to estimate the torque generated by individual F_1 molecules from the hydrodynamic friction that should be in equilibrium with F_1's torque. The torque was determined to be around 40 pN nm. Although this is a rough estimation without
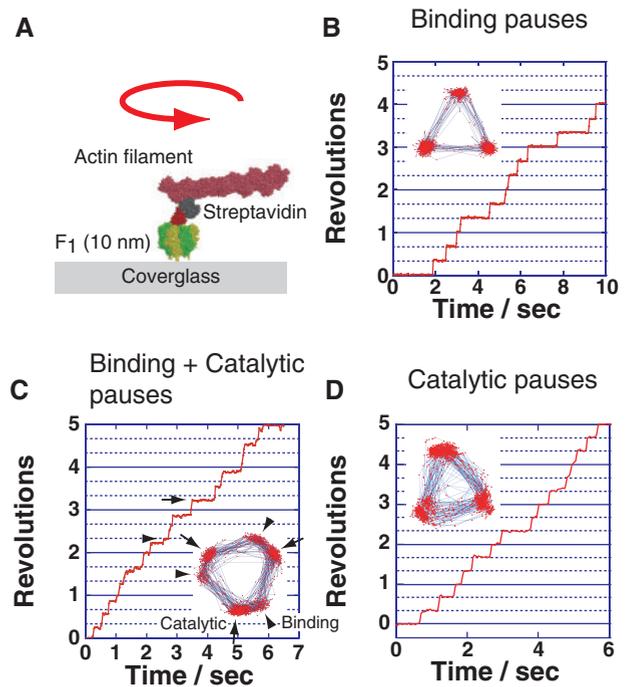
Fig. 3 Single-molecule rotation assay of F_1. (A) A schematic image of the experimental setup. The $α_3β_3$-ring is fixed on the glass surface to suppress translational and rotational Brownian motion of the F_1 molecule. A rotation probe (fluorescently-labelled actin filament) is attached to the γ-subunit to visualize the rotary motion under an optical microscope. (B) Rotation of F_1-ATPase under ATP-limiting conditions (60 nM ATP). Inset shows the trajectory of the centroid of the probe. (C) Rotation of mutant F_1-ATPase, β(E190D), at 2 μM ATP. Under this condition, 120° step is divided into 0° and 80° dwelling positions. Each pause corresponds to ATP binding and ATP catalytic dwelling positions, respectively. Arrow heads and arrows indicate the positions of ATP binding and catalytic dwell, respectively. (D) Rotation of a mutant F_1-ATPase, β(E190D), at saturating ATP (2 mM). Hydrolysis rate is slowed by the mutation so that three pauses to wait for the hydrolysis reaction are observed.

consideration of the viscosity increment in the immediate vicinity of surface, the value was recently confirmed to be valid using more precise torque measurements based on fluctuation theorem, which estimates the entropy generation upon the rotation without assuming the friction coefficient (32). Taking into account that the step size is 120°, each coupled with single ATP hydrolysis turnover as below, F_1 works with 80 pN nm, which corresponds to the free energy released from hydrolysis of a single ATP molecule under physiological conditions, suggesting high 100% energy conversion efficiency of F_1.

Stepping rotation of F_1

Many attempts have been made to resolve rotary motion into discrete steps to clarify how the rotation is coupled with each elementary catalytic step of ATP hydrolysis: ATP-binding, hydrolysis and product release. The stepping rotation was first observed in the rotation assay with actin filaments under ATP-limiting conditions, where the ATP-binding process determines the net turnover rate of ATP hydrolysis and rotation.

When [ATP] is well below the Michaelis–Menten constant (K_M) of the rotation (∼1 µM), F_1 showed discrete 120° steps that were intervened with pauses, consistent with the pseudo 3-fold symmetry of the $\alpha_3\beta_3$-ring (Fig. 3B). The mean dwell time of the pause before the steps was inversely proportional to [ATP], suggesting that each step is triggered by a single event of ATP binding. A histogram of the dwell time showed an exponential decay with the time constant in consistent with the observed mean dwell time, implying that the single event triggers the 120° step (*33*). The coupling ratio of a single 120° step per ATP was directly confirmed in a later study (*34*). However, the stepping rotation was not detected at ATP-saturating conditions owing to damping by high viscous friction against actin filaments. Therefore, a very small probe was employed to detect the intrinsic stepping motion of F_1. A single gold colloid (40 nm) was attached to the γ-subunit so that viscous friction was negligible, and the maximum rotational velocity reached and exceeded the expected rate from bulk ATPase (*35*). The discrepancy from bulk ATPase is attributed to some fraction of F_1 being in an inactive state, the so-called ADP-inhibited form (*36*), in the ensemble measurement. In this rotation assay, the 120° step rotation was observed even under ATP-saturating conditions. Near the K_M, where time constants for the ATP-binding step and other catalytic steps are comparable, the rotation showed two substeps of which angular displacement were resolved into 90° and 30° (*35*). In a following experiment, in order to facilitate the analysis of the catalytic dwell, a mutation was introduced at the catalytic site, βE190D (thermophilic *Bacillus* PS3) that significantly slows the rate constant of hydrolysis step (*37*). Around K_M, the mutant F_1 shows six pauses composed of 0° and 80° dwelling positions during rotation, revising the substep sizes to be 80° and 40° (Fig. 3C). Kinetic analyses of the dwell time at 0° and 80° dwelling positions revealed that these substeps are triggered by ATP binding and two consecutive reactions with time constants around 1 ms, respectively. Recent studies have revised the two time constants at 80° dwelling position to be 1.3 ms and ∼0.1–0.3 ms (*38, 39*). One of the two reactions at 80° dwelling position was revealed to be the hydrolysis step in the experiment that employed the aforementioned mutant F_1 with slow hydrolysis rate and a slowly hydrolysing ATP analogue adenosine 5′-(γ-thio)triphosphate (ATPγS) (*37*). The angular dwelling positions at 0° and 80° are, therefore, termed the binding angle and catalytic angle (Fig. 3C and D), respectively. The angular positions of product release were investigated by adding an excess of ADP or P_i in the solution (*38, 40*). In the presence of ADP, the rotation was slowed because of lengthening of the dwell time at the binding angle, suggesting that the ADP-releasing angle is at a binding angle. Simultaneous imaging of fluorescently labelled nucleotide with the γ rotation also verified this point: fluorescently labelled ATP is released presumably as ADP after the γ-subunit rotates 240° or more from the angle where the nucleotide is bound to F_1. In contrast, in the presence of P_i, F_1 showed longer pauses at the catalytic

angle. Thus, it is thought that the release of ADP and P_i occurs at the binding and catalytic angles, respectively. Another intermediate of F_1 at the binding angle was unexpectedly found in the rotation assay at low temperature, ∼4°C (*40*). This reaction showed an extremely high Q_{10} factor of 19, so this reaction is termed the temperature-sensitive reaction (TS). A direct correlation between TS and the ATP-binding or ADP-release step was not found although TS takes place at the binding. Considering the high Q_{10} factor, TS reaction might be some conformational rearrangement before or after ATP binding (*41*).

Reaction scheme of F_1-ATPase

As mentioned above, all of the elementary reaction steps were identified to occur at the binding angle or catalytic angle. However, because there are three positions for binding and catalytic angles, it is required for the establishment of the reaction scheme of F_1 to determine at which angle each reaction occurs. ADP release was shown to occur at 240–320°, but most likely at 240°. The angle for hydrolysis was determined using a hybrid F_1 carrying a single copy of the aforementioned mutant β-subunit, βE190D (*42*). This hybrid allows us to identify the hydrolysis angle because the incorporated mutant β-subunit shows distinctly long pauses at two positions. One is at the ATP-binding angle of the mutant β-subunit (0°), and the other one is at +200° from the binding angle. Thus, the hydrolysis angle was determined to be 200°. Note that the pause at 0° is due to the TS intermediate state (*41*), although it was attributed to ATP waiting dwell in the original report (*43*). The TS dwell could be confounded as the 320° pause presumably due to experimental error. The timing of P_i release has recently been determined to be at 320° in another type of experiment (*39*) where F_1 was stalled with magnetic tweezers during hydrolysis dwell that was lengthened by βE190D and/or ATPγS. On the basis of the observation that bound ATP or ATPγS undergoes hydrolysis and synthesis in a reversible manner, it was shown that P_i (or thiophosphate) is not released immediately after hydrolysis at 200°. Because the P_i release has to be after hydrolysis and at a catalytic angle, it was concluded that P_i release occurs at 320°. Thus, the present reaction scheme of rotation and catalysis is as follows: ATP binding at 0°, hydrolysis at 200°, ADP release 240° and P_i release at 320° (Fig. 4).

Correlation of reaction scheme with crystal structure

While the single-molecule rotation assay revealed that F_1 has two stable conformations in pausing at the binding or catalytic angle, current crystal structures show essentially a single conformation. Correlation with the crystal structure remained obscure, although the interpretation of the crystal structure is crucial, especially for theoretical studies. Therefore, attempts have been made to determine whether the crystal structure represents the binding dwell or catalytic dwell
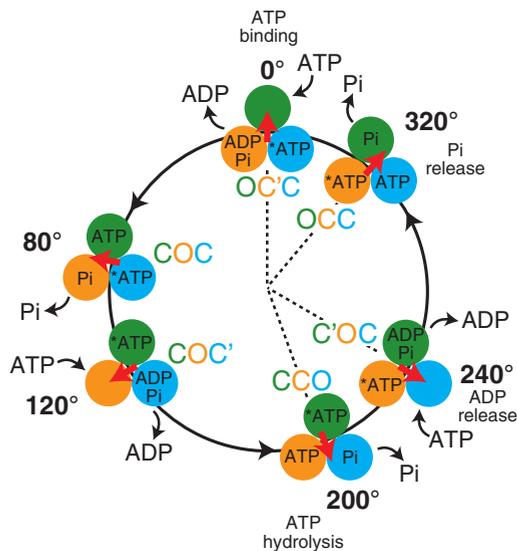
Fig. 4 Mechanochemical coupling scheme of F_1. Each circle represents the chemical state of the catalytic sites on the β-subunit. The red arrow represents the angular position of the γ-subunit. O, C′ and C indicate the open, half-closed and closed forms, respectively. The green catalytic site retains the bound nucleotide as ATP until the γ-subunit rotates 200° from the binding angle (0°). At 200°, the catalytic site hydrolyses ATP into ADP and P_i, each of which is released at 240° and 320°, respectively. The conformation of the β-subunit changes from open to closed upon ATP binding and remains in the closed form until the γ-subunit rotates 240°. At 240°, this β-subunit moves to the half-closed form, and then it returns to the open form with accompanying rotation of the γ-subunit.

(28, 44, 45). On the basis of the crystal structure, the characteristic interaction with the γ-subunit was identified in the $β_{DP}$ form. Cysteine residues were genetically incorporated into the residues involved in the direct β-γ contact. The mutant F_1 was analysed in the rotation assay. During observation, incorporated cysteine residues were cross-linked through disulphide bonds by infusing an oxidizing buffer to stall F_1 in the crystal structure form. The pausing angle corresponded to the catalytic angle. Thus, it was shown that the crystal structure represents the catalytic dwelling state and that $β_{TP}$, $β_{DP}$ and $β_{Empty}$ correspond to the 80°, 200° and 320° state, respectively (Fig. 4, green circles). These data were supported by experiments by Masaike *et al.* where the C-terminal domain of the β-subunit that undergoes the large swing motion upon ATP binding was labelled with a fluorescent dye (28). The observed angular positions in the catalytic dwell corresponded to those observed in the crystal structure. Interestingly, they found that at 240°, the β-subunit takes a new conformation, which they termed 'half-closed', while at other binding angles, the β-subunit takes the same conformation as the catalytic angles: open at 0° and closed at 120° (Fig. 4).

ATP synthesis upon reverse rotation of F_1

Although the essential properties and basic mechanochemical coupling scheme of F_1 as an ATP-driven motor have been established, the physiological role of F_oF_1-ATP synthase, that is ATP synthesis, has not

been sufficiently studied in single-molecule experiments. If ATP synthesis is a simple reverse reaction of hydrolysis, forcibly reversing rotation of F_1 should lead to efficient ATP synthesis. Two lines of single-molecule experiments have been carried out to investigate this hypothesis. In the first experiment (46), a large number of F_1 molecules were enclosed in an observation chamber and forcibly rotated in the reverse direction with a magnetic bead tweezer system. The synthesized ATP was detected as bioluminescence using the luciferin–luciferase system. Although ATP synthesis upon reverse rotation was clearly demonstrated, the uncertainty of the number of active F_1 molecules in the chamber did not allow a quantitative estimation of the mechanochemical coupling ratio. Therefore, the following experiment focused a single active F_1 molecule to determine the coupling ratio (34). The technical issue to be addressed was detection of a very small number of ATP molecules generated from a single F_1 molecule. Even if we assume that F_1 synthesizes three ATP molecules per one revolution at 10 Hz for 1 min, the total number of ATP molecule is only 1,800 molecules (3.0×10^{-21} mol), which is far below the detection limit of the luciferase assay. To address this issue, a microscopic reaction chamber system was developed using a microfabrication technique, which has identically shaped reaction chambers, each of which is a few microns in scale and has a volume of 6 fL (47). Because the extremely small reaction volume resulted in high concentration, it was possible to detect a small amount of reaction product yielded from a single enzyme molecule. A single F_1 molecule was encapsulated in the microchamber to accumulate synthesized ATP molecules (Fig. 5A and B). After forcible reverse rotation with magnetic tweezers, F_1 was released from the tweezers. Because the rotational rate of ATP-driven rotation is proportional to [ATP] under the experimental conditions, one can measure the increment of [ATP] as that of the ATP-driven rotation rate. It was found that while the $α_3β_3γ$ subcomplex showed very weak ATP synthesis activity, the $α_3β_3γε$ subcomplex had highly efficient ATP synthesis, up to ∼80% (2.3 ATP molecules per turn) (Fig. 5C). It is likely that the ε-subunit stabilizes the protruding portion of the γ-subunit, as seen in the crystal structure, to transmit the applied torque to γ. This result implies that the efficiency of the mechanochemical coupling in ATP synthesis is also high in the whole F_oF_1 complex. High reversibility of mechanochemical coupling is a remarkable feature of the ATP synthase that distinguishes it from other molecular motors; other motor proteins such as kinesin and myosin do not synthesize ATP when the movements are reversed by external force.
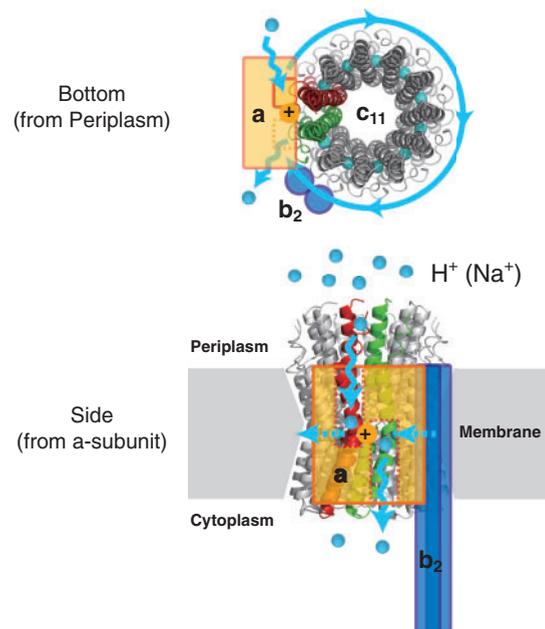
Structure of F_o

Bacterial F_o has the common and simple subunit stoichiometry of ab_2c_{10-15}, while mitochondrial F_o has additional subunits: *d*, *e*, *f*, *OSCP*, *F6* and *A6L* (48). We hereafter focus on the minimum subcomplex of F_o, ab_2c_{10-15}. The structure of the *c* subunit was first resolved in a monomer state by NMR (49). The *c*
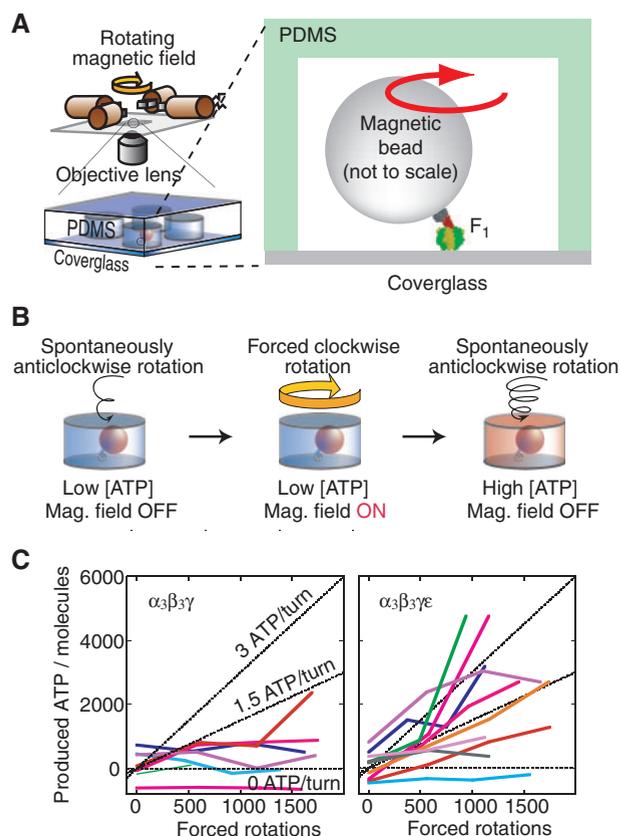
Fig. 5 ATP synthesis by reversing F_1. (A) Schematic drawing of experimental setup. (B) Experimental procedure of ATP synthesis. Active single F_1 is enclosed in a femtolitre chamber (left). A magnetic bead attached to the γ-subunit is forcibly rotated by magnetic tweezers (centre). Newly synthesized ATP is accumulated in the chamber. The number of synthesized ATP molecules is determined from the increments in the ATP-driven rotational speed of released F_1 (right). (C) ATP synthesis by reversing $\alpha_3\beta_3\gamma$ (left) and $\alpha_3\beta_3\gamma\varepsilon$ (right). Each trace is derived from individual F_1 molecules. Dotted lines indicate slopes of the coupling ratio of 0% (0 ATP/turn), 50% (1.5 ATP/turn) and 100% (3 ATP/turn).

Fig. 6 Structure of F_o. The c_{10}-ring is from the crystal structure of Na$^+$-transport F_o from *Ilyobacter tartaricus* (PDB code; 1YCE). The blue spheres at the middle of the c_{10}-ring represent bound Na$^+$ ions. Schematic image of stator ab_2 complex (thin orange and blue) is constructed based on the two-channel model. One half channel is exposed to the periplasmic side and the other to cytoplasmic side. Rotation of the c-ring accompanies the proton-transfer between the a and c subunits. Two c subunit monomers at the interface of the a subunit are shown in red and green, respectively. The shortcut transfer of protons between the c subunits connected to the half channels are blocked with the positive charge of the conserved Arg residue of the a subunit (depicted as the plus symbol).

subunit has a hairpin structure that is composed of two α-helices and a connecting loop. Crystal structures of the F_1–c-ring structure (*10*, *11*) and isolated c-ring (*14–17*, *19–21*) revealed that the c subunits form a ring complex by assembling in a circle with the C-terminus pointing outwards and the connecting loop towards the F_1 side (cytoplasmic side in bacteria) (Fig. 6). The b subunit has an N-terminal transmembrane domain. The b subunit forms a homodimer (*50*) which functions as the peripheral stalk to hold the stator parts of F_1 and F_o to avoid slippage. It was shown that the b subunit has robustness against extensive deletion and insertion at the cytoplasmic helix (*51*, *52*), suggesting that the b_2 dimer also acts as the elastic connector for smooth torque transmission. The structure of the a subunit remains unclear. It is thought that this subunit has five transmembrane helices (*53–55*). Because the cavity of the c-ring is too small to accommodate the a subunit and/or the b_2 dimer, each of which has five or two helices, it is reasonable to assume that the ab_2 complex resides outside of the c-ring (*56*, *57*).

Proton translocation pathway of F_o: the 2-channel model

The mechanical rotation of the c-ring by F_o is driven by proton flow through F_o. Although the structural basis of the proton translocation pathway is unknown, extensive biochemical work on F_o subunits has identified several charged residues in the transmembrane helices of the a and c subunits that would be directly involved in proton translocation. Among them, Asp or Glu of the c subunit and Arg of the a subunit, which correspond to cAsp61 and aArg210 of *E. coli* F_o, are highly conserved among species and thought to have crucial roles in proton translocation. The crystal structure of the c-ring showed that the Asp residue (Glu in *I. tartaricus* F_o) of the c subunit resides at the middle of the C-terminal helix. The recent structure of the c_{10}-ring from *I. tartaricus* F_o, which is a Na$^+$-transporting F_o, revealed that the Glu residues are occupied with Na$^+$ ions (Fig. 6). Thus, it is well established that this conserved carboxyl residue is one of the proton-binding sites. However, other charged residues are not found in the c subunit in the vicinity of the carboxyl residue, suggesting that the a subunit has proton translocation pathways. The most widely accepted model on proton translocation in F_o is the so-called two-channel model, which assumes that the a subunit possesses two proton pathways each of which spans half of the membrane, but towards different sides;

the channels connect the proton-binding site of the *c* subunit with the periplasmic or cytoplasmic space (*58–60*) (Fig. 6). Notice each channel has contact with a different *c* subunit, which are adjacent to each other. In other words, the *a* subunit interacts with two *c* subunits, each contacting *via* a different half channel. The proposed mechanism of proton transfer in ATP synthesis mode is as follows (*60–62*): a proton enters the half channel exposed to the periplasmic side (or intermembrane space of mitochondria) and is then transferred to the carboxy residue of the *c* subunit. This protonation neutralizes the negative charge of the residue, allowing the *c* subunit to rotate apart from the *a* subunit towards the surrounding lipid layer. At the same time, the neighbouring *c* subunit at the anticlockwise side returns from the lipid layer to form contacts with the other half channel, which has a hydrophilic environment to promote deprotonation of the carboxyl residue. The released proton then enters into the cytoplasmic space. The role of the conserved Arg in the *a* subunit is likely to block the futile rotation of the *c* subunit without deprotonation by attracting only the deprotonated *c* subunit with its positive charge (*62, 63*). In the ATP-driven proton-pumping mode, the sequence of events is reversed.

Rotation of *c*-ring in F_o

After the direct observation of F_1, the verification of the *c*-ring rotation against the ab_2 complex became an important issue. Although around 10 years have passed since the verification of the *c*-ring rotation, little progress has been made on the rotary dynamics of F_o, compared with F_1, owing to challenges in handling the complicated membrane system and difficulty in stably charging the membrane potential high enough to reverse F_1. Although detergent-solubilized F_oF_1 was subjected to the rotation assay in ATP hydrolysis conditions in early studies (*64, 65*), the observed rotation was insensitive to the gold-standard inhibitor of F_o, dicyclohexyl-carbodiimide (DCCD), implying that the observed rotating is not coupled with the proton translocation of F_o (*64, 66*). The subunit interactions of F_o are weakened in the presence of detergent, which often causes subunit dissociation in biochemical assays (*67*). Actually, it has been later reported that the rotation in this system is insensitive to mutation at the conserved Arg of the *a* subunit (*68*). Verification of the *c*-ring rotation came from biochemical experiments showing that crosslinkage of the *c*-ring with the rotor subunits of F_1 ($γ$ and $ε$ subunits) does not diminish ATP synthesis activity (*69*), while the *a–c* crosslink abolishes ATPase activity coupled with proton translocation (*70*). Further verification was made by detection of the exchanged cross-link product between the *a* and *c* subunits, which was probed with a ^{14}C-labelled *c* subunit (*71*). Single-molecule imaging of rotation under ATP synthesis conditions has also been attempted. The rotation of F_oF_1 reconstituted in liposome was detected from the dipole moment angle of the fluorescent marker dye incorporated into a rotor subunit (*72*) or Förster

resonance energy transfer (FRET) efficiency between two fluorescent dyes introduced into the stator and rotor subunits (*73*). A drawback of these experiments is that the membrane potential is transient and, therefore, it is very difficult to correlate the observed rotational velocity with the membrane potential. However, one essential property of F_o rotation was revealed with the FRET experiment: multiple stepping rotation was detected that was interpreted as $36°$ steps based on the 10-fold symmetry of the rotor (*74*). The $36°$ stepping rotation was later proved in the rotation assay under ATP hydrolysis conditions where a gold nanorod was used as the rotation probe (*75*). F_oF_1 was reconstituted into a nanodisc of lipid bilayer, and the rotation was monitored from the angle of polarized scattered light along the long axis of the nanorod. However, understanding the dynamics of F_o rotation is still in its early stages. Experimental systems that allow stable charging of the membrane potential simultaneously with observation of F_1 rotation with high spatiotemporal resolution are highly awaited.

Acknowledgements

Conflict of Interest
None declared.

References

1. Yoshida, M., Muneyuki, E., and Hisabori, T. (2001) ATP synthase–a marvellous rotary engine of the cell. *Nat. Rev. Mol. Cell. Biol.* **2**, 669–677
2. Kato, Y., Matsui, T., Tanaka, N., Muneyuki, E., Hisabori, T., and Yoshida, M. (1997) Thermophilic F1-ATPase is activated without dissociation of an endogenous inhibitor, epsilon subunit. *J. Biol. Chem.* **272**, 24906–24912
3. Smith, J.B. and Sternweis, P.C. (1977) Purification of membrane attachment and inhibitory subunits of the proton translocating adenosine triphosphatase from Escherichia coli. *Biochemistry* **16**, 306–311
4. Sternweis, P.C. and Smith, J.B. (1980) Characterization of the inhibitory (epsilon) subunit of the proton-translocating adenosine triphosphatase from Escherichia coli. *Biochemistry* **19**, 526–531
5. Iino, R., Murakami, T., Iizuka, S., Kato-Yamada, Y., Suzuki, T., and Yoshida, M. (2005) Real-time monitoring of conformational dynamics of the epsilon subunit in F1-ATPase. *J. Biol. Chem.* **280**, 40130–40134
6. Saita, E., Iino, R., Suzuki, T., Feniouk, B.A., Kinosita, K. Jr., and Yoshida, M. (2010) Activation and stiffness of the inhibited states of F1-ATPase probed by single-molecule manipulation. *J. Biol. Chem.* **285**, 11411–11417
7. Suzuki, T., Murakami, T., Iino, R., Suzuki, J., Ono, S., Shirakihara, Y., and Yoshida, M. (2003) F0F1-ATPase/synthase is geared to the synthesis mode by

conformational rearrangement of epsilon subunit in response to proton motive force and ADP/ATP balance. *J. Biol. Chem.* **278**, 46840–46846

8. Iino, R., Hasegawa, R., Tabata, K.V., and Noji, H. (2009) Mechanism of inhibition by C-terminal alpha-helices of the epsilon subunit of Escherichia coli FoF1-ATP synthase. *J. Biol. Chem.* **284**, 17457–17464

9. Feniouk, B.A., Suzuki, T., and Yoshida, M. (2006) The role of subunit epsilon in the catalysis and regulation of FOF1-ATP synthase. *Biochim. Biophys. Acta* **1757**, 326–338

10. Watt, I.N., Montgomery, M.G., Runswick, M.J., Leslie, A.G., and Walker, J.E. (2010) Bioenergetic cost of making an adenosine triphosphate molecule in animal mitochondria. *Proc. Natl Acad. Sci. USA* **107**, 16823–16827

11. Stock, D., Leslie, A.G., and Walker, J.E. (1999) Molecular architecture of the rotary motor in ATP synthase. *Science.* **286**, 1700–1705

12. Jiang, W., Hermolin, J., and Fillingame, R.H. (2001) The preferred stoichiometry of c subunits in the rotary motor sector of Escherichia coli ATP synthase is 10. *Proc. Natl Acad. Sci. USA* **98**, 4966–4971

13. Mitome, N., Suzuki, T., Hayashi, S., and Yoshida, M. (2004) Thermophilic ATP synthase has a decamer c-ring: indication of noninteger 10:3 H+/ATP ratio and permissive elastic coupling. *Proc. Natl Acad. Sci. USA* **101**, 12159–12164

14. Meier, T., Polzer, P., Diederichs, K., Welte, W., and Dimroth, P. (2005) Structure of the rotor ring of F-Type Na+-ATPase from Ilyobacter tartaricus. *Science* **308**, 659–662

15. Stahlberg, H., Muller, D.J., Suda, K., Fotiadis, D., Engel, A., Meier, T., Matthey, U., and Dimroth, P. (2001) Bacterial Na(+)-ATP synthase has an undecameric rotor. *EMBO Rep.* **2**, 229–233

16. Meier, T., Matthey, U., von Ballmoos, C., Vonck, J., Krug von Nidda, T., Kuhlbrandt, W., and Dimroth, P. (2003) Evidence for structural integrity in the undecameric c-rings isolated from sodium ATP synthases. *J. Mol. Biol.* **325**, 389–397

17. Meier, T., Ferguson, S.A., Cook, G.M., Dimroth, P., and Vonck, J. (2006) Structural investigations of the membrane-embedded rotor ring of the F-ATPase from Clostridium paradoxum. *J. Bacteriol.* **188**, 7759–7764

18. Meier, T., Morgner, N., Matthies, D., Pogoryelov, D., Keis, S., Cook, G.M., Dimroth, P., and Brutschy, B. (2007) A tridecameric c ring of the adenosine triphosphate (ATP) synthase from the thermoalkaliphilic Bacillus sp. strain TA2.A1 facilitates ATP synthesis at low electrochemical proton potential. *Mol. Microbiol.* **65**, 1181–1192

19. Preiss, L., Yildiz, O., Hicks, D.B., Krulwich, T.A., and Meier, T. (2010) A new type of proton coordination in an F(1)F(o)-ATP synthase rotor ring. *PLoS Biol.* **8**, e1000443

20. Seelert, H., Poetsch, A., Dencher, N.A., Engel, A., Stahlberg, H., and Muller, D.J. (2000) Structural biology. Proton-powered turbine of a plant motor. *Nature* **405**, 418–419

21. Pogoryelov, D., Yu, J., Meier, T., Vonck, J., Dimroth, P., and Muller, D.J. (2005) The c15 ring of the Spirulina platensis F-ATP synthase: F1/F0 symmetry mismatch is not obligatory. *EMBO Rep.* **6**, 1040–1044

22. Diez, M., Zimmermann, B., Borsch, M., Konig, M., Schweinberger, E., Steigmiller, S., Reuter, R., Felekyan, S., Kudryavtsev, V., Seidel, C.A., and Graber, P. (2004) Proton-powered subunit rotation in single membrane-bound F0F1-ATP synthase. *Nat. Struct. Mol. Biol.* **11**, 135–141

23. Boyer, P.D. (1997) The ATP synthase–a splendid molecular machine. *Annu Rev Biochem.* **66**, 717–749

24. Wakabayashi, T., Kubota, M., Yoshida, M., and Kagawa, Y. (1977) Structure of ATPase (coupling factor TF1) from a thermophilic bacterium. *J. Mol. Biol.* **117**, 515–519

25. Kagawa, Y., Sone, N., Yoshida, M., Hirata, H., and Okamoto, H. (1976) Proton translocating ATPase of a thermophilic bacterium. Morphology, subunits, and chemical composition. *J. Biochem* **80**, 141–151

26. Yoshida, M., Sone, N., Hirata, H., and Kagawa, Y. (1975) A highly stable adenosine triphosphatase from a thermophillie bacterium. Purification, properties, and reconstitution. *J. Biol. Chem.* **250**, 7910–7916

27. Abrahams, J.P., Leslie, A.G., Lutter, R., and Walker, J.E. (1994) Structure at 2.8 A resolution of F1-ATPase from bovine heart mitochondria. *Nature* **370**, 621–628

28. Masaike, T., Koyama-Horibe, F., Oiwa, K., Yoshida, M., and Nishizaka, T. (2008) Cooperative three-step motions in catalytic subunits of F(1)-ATPase correlate with 80 degrees and 40 degrees substep rotations. *Nat. Struct. Mol. Biol.* **15**, 1326–1333

29. Duncan, T.M., Bulygin, V.V., Zhou, Y., Hutcheon, M.L., and Cross, R.L. (1995) Rotation of subunits during catalysis by Escherichia coli F1-ATPase. *Proc. Natl Acad. Sci. USA* **92**, 10964–10968

30. Sabbert, D., Engelbrecht, S., and Junge, W. (1996) Intersubunit rotation in active F-ATPase. *Nature* **381**, 623–625

31. Noji, H., Yasuda, R., Yoshida, M., and Kinosita, K. Jr. (1997) Direct observation of the rotation of F1-ATPase. *Nature* **386**, 299–302

32. Hayashi, K., Ueno, H., Iino, R., and Noji, H. (2010) Fluctuation theorem applied to F1-ATPase. *Phys. Rev. Lett.* **104**, 218103

33. Yasuda, R., Noji, H., Kinosita, K. Jr., and Yoshida, M. (1998) F1-ATPase is a highly efficient molecular motor that rotates with discrete 120 degree steps. *Cell* **93**, 1117–1124

34. Rondelez, Y., Tresset, G., Nakashima, T., Kato-Yamada, Y., Fujita, H., Takeuchi, S., and Noji, H. (2005) Highly coupled ATP synthesis by F1-ATPase single molecules. *Nature* **433**, 773–777

35. Yasuda, R., Noji, H., Yoshida, M., Kinosita, K. Jr., and Itoh, H. (2001) Resolution of distinct rotational substeps by submillisecond kinetic analysis of F1-ATPase. *Nature* **410**, 898–904

36. Hirono-Hara, Y., Noji, H., Nishiura, M., Muneyuki, E., Hara, K.Y., Yasuda, R., Kinosita, K. Jr., and Yoshida, M. (2001) Pause and rotation of F(1)-ATPase during catalysis. *Proc. Natl Acad. Sci. USA* **98**, 13649–13654

37. Shimabukuro, K., Yasuda, R., Muneyuki, E., Hara, K.Y., Kinosita, K. Jr., and Yoshida, M. (2003) Catalysis and rotation of F1 motor: cleavage of ATP at the catalytic site occurs in 1 ms before 40 degree substep rotation. *Proc. Natl Acad. Sci. USA* **100**, 14731–14736

38. Adachi, K., Oiwa, K., Nishizaka, T., Furuike, S., Noji, H., Itoh, H., Yoshida, M., and Kinosita, K. Jr. (2007) Coupling of rotation and catalysis in F(1)-ATPase revealed by single-molecule imaging and manipulation. *Cell* **130**, 309–321

39. Watanabe, R., Iino, R., and Noji, H. (2010) Phosphate release in F1-ATPase catalytic cycle follows ADP release. *Nat. Chem. Biol.* **6**, 814–820

40. Watanabe, R., Iino, R., Shimabukuro, K., Yoshida, M., and Noji, H. (2008) Temperature-sensitive reaction intermediate of F1-ATPase. *EMBO Rep.* **9**, 84–90

41. Enoki, S., Watanabe, R., Iino, R., and Noji, H. (2009) Single-molecule study on the temperature-sensitive reaction of F1-ATPase with a hybrid F1 carrying a single beta(E190D). *J. Biol. Chem.* **284**, 23169–23176

42. Ariga, T. (2008) The concerted nature between three catalytic subunits driving the F1 rotary motor. *Biosystems* **93**, 68–77

43. Ariga, T., Muneyuki, E., and Yoshida, M. (2007) F1-ATPase rotates by an asymmetric, sequential mechanism using all three catalytic subunits. *Nat. Struct. Mol. Biol.* **14**, 841–846

44. Okuno, D., Ikeguchi, M., and Noji, H. (2010) Measurement of the conformational state of F(1)-ATPase by single-molecule rotation. *Methods Enzymol.* **475**, 279–296

45. Sielaff, H., Rennekamp, H., Engelbrecht, S., and Junge, W. (2008) Functional halt positions of rotary FOF1-ATPase correlated with crystal structures. *Biophys. J.* **95**, 4979–4987

46. Itoh, H., Takahashi, A., Adachi, K., Noji, H., Yasuda, R., Yoshida, M., and Kinosita, K. (2004) Mechanically driven ATP synthesis by F1-ATPase. *Nature* **427**, 465–468

47. Rondelez, Y., Tresset, G., Tabata, K.V., Arata, H., Fujita, H., Takeuchi, S., and Noji, H. (2005) Microfabricated arrays of femtoliter chambers allow single molecule enzymology. *Nat. Biotechnol.* **23**, 361–365

48. Collinson, I.R., van Raaij, M.J., Runswick, M.J., Fearnley, I.M., Skehel, J.M., Orriss, G.L., Miroux, B., and Walker, J.E. (1994) ATP synthase from bovine heart mitochondria. In vitro assembly of a stalk complex in the presence of F1-ATPase and in its absence. *J. Mol. Biol.* **242**, 408–421

49. Girvin, M.E., Rastogi, V.K., Abildgaard, F., Markley, J.L., and Fillingame, R.H. (1998) Solution structure of the transmembrane H+-transporting subunit c of the F1F0 ATP synthase. *Biochemistry* **37**, 8817–8824

50. Dunn, S.D., McLachlin, D.T., and Revington, M. (2000) The second stalk of Escherichia coli ATP synthase. *Biochim. Biophys. Acta* **1458**, 356–363

51. Sorgen, P.L., Bubb, M.R., and Cain, B.D. (1999) Lengthening the second stalk of F(1)F(0) ATP synthase in Escherichia coli. *J. Biol. Chem.* **274**, 36261–36266

52. Sorgen, P.L., Caviston, T.L., Perry, R.C., and Cain, B.D. (1998) Deletions in the second stalk of F1F0-ATP synthase in Escherichia coli. *J. Biol. Chem.* **273**, 27873–27878

53. Long, J.C., Wang, S., and Vik, S.B. (1998) Membrane topology of subunit a of the F1F0 ATP synthase as determined by labeling of unique cysteine residues. *J. Biol. Chem.* **273**, 16235–16240

54. Valiyaveetil, F.I. and Fillingame, R.H. (1998) Transmembrane topography of subunit a in the Escherichia coli F1F0 ATP synthase. *J. Biol. Chem.* **273**, 16241–16247

55. Wada, T., Long, J.C., Zhang, D., and Vik, S.B. (1999) A novel labeling approach supports the five-transmembrane model of subunit a of the Escherichia coli ATP synthase. *J. Biol. Chem.* **274**, 17353–17357

56. Rubinstein, J.L., Walker, J.E., and Henderson, R. (2003) Structure of the mitochondrial ATP synthase by electron cryomicroscopy. *EMBO J.* **22**, 6182–6192

57. Takeyasu, K., Omote, H., Nettikadan, S., Tokumasu, F., Iwamoto-Kihara, A., and Futai, M. (1996) Molecular imaging of Escherichia coli F0F1-ATPase in reconstituted membranes using atomic force microscopy. *FEBS Lett.* **392**, 110–113

58. Elston, T., Wang, H., and Oster, G. (1998) Energy transduction in ATP synthase. *Nature* **391**, 510–513

59. Junge, W., Lill, H., and Engelbrecht, S. (1997) ATP synthase: an electrochemical transducer with rotatory mechanics. *Trends Biochem. Sci.* **22**, 420–423

60. Vik, S.B. and Antonio, B.J. (1994) A mechanism of proton translocation by F1F0 ATP synthases suggested by double mutants of the a subunit. *J. Biol. Chem.* **269**, 30364–30369

61. Dimroth, P., von Ballmoos, C., and Meier, T. (2006) Catalytic and mechanical cycles in F-ATP synthases. Fourth in the Cycles Review Series. *EMBO Rep.* **7**, 276–282

62. Oster, G. and Wang, H. (2003) Rotary protein motors. *Trends Cell Biol.* **13**, 114–121

63. Mitome, N., Ono, S., Sato, H., Suzuki, T., Sone, N., and Yoshida, M. (2010) Essential arginine residue of the F(o)-a subunit in F(o)F(1)-ATP synthase has a role to prevent the proton shortcut without c-ring rotation in the F(o) proton channel. *Biochem J.* **430**, 171–177

64. Panke, O., Gumbiowski, K., Junge, W., and Engelbrecht, S. (2000) F-ATPase: specific observation of the rotating c subunit oligomer of EF(o)EF(1). *FEBS Lett.* **472**, 34–38

65. Sambongi, Y., Iko, Y., Tanabe, M., Omote, H., Iwamoto-Kihara, A., Ueda, I., Yanagida, T., Wada, Y., and Futai, M. (1999) Mechanical rotation of the c subunit oligomer in ATP synthase (F0F1): direct observation. *Science* **286**, 1722–1724

66. Tanabe, M., Nishio, K., Iko, Y., Sambongi, Y., Iwamoto-Kihara, A., Wada, Y., and Futai, M. (2001) Rotation of a complex of the gamma subunit and c ring of Escherichia coli ATP synthase. The rotor and stator are interchangeable. *J. Biol. Chem.* **276**, 15269–15274

67. Tsunoda, S.P., Aggeler, R., Noji, H., Kinosita, K. Jr., Yoshida, M., and Capaldi, R.A. (2000) Observations of rotation within the F(o)F(1)-ATP synthase: deciding between rotation of the F(o)c subunit ring and artifact. *FEBS Lett.* **470**, 244–248

68. Hosokawa, H., Nakanishi-Matsui, M., Kashiwagi, S., Fujii-Taira, I., Hayashi, K., Iwamoto-Kihara, A., Wada, Y., and Futai, M. (2005) ATP-dependent rotation of mutant ATP synthases defective in proton transport. *J. Biol. Chem.* **280**, 23797–23801

69. Tsunoda, S.P., Aggeler, R., Yoshida, M., and Capaldi, R.A. (2001) Rotation of the c subunit oligomer in fully functional F1Fo ATP synthase. *Proc. Natl Acad. Sci. USA* **98**, 898–902

70. Suzuki, T., Ueno, H., Mitome, N., Suzuki, J., and Yoshida, M. (2002) F(0) of ATP synthase is a rotary proton channel. Obligatory coupling of proton translocation with rotation of c-subunit ring. *J. Biol. Chem.* **277**, 13281–13285

71. Hutcheon, M.L., Duncan, T.M., Ngai, H., and Cross, R.L. (2001) Energy-driven subunit rotation at the interface between subunit a and the c oligomer in the F(O) sector of Escherichia coli ATP synthase. *Proc. Natl Acad. Sci. USA* **98**, 8519–8524

72. Kaim, G., Prummer, M., Sick, B., Zumofen, G., Renn, A., Wild, U.P., and Dimroth, P. (2002) Coupled rotation

within single F0F1 enzyme complexes during ATP synthesis or hydrolysis. *FEBS Lett.* **525**, 156−163

73. Borsch, M., Diez, M., Zimmermann, B., Reuter, R., and Graber, P. (2002) Stepwise rotation of the gamma-subunit of EF(0)F(1)-ATP synthase observed by intramolecular single-molecule fluorescence resonance energy transfer. *FEBS Lett.* **527**, 147−152

74. Duser, M.G., Zarrabi, N., Cipriano, D.J., Ernst, S., Glick, G.D., Dunn, S.D., and Borsch, M. (2009) 36 degrees step size of proton-driven c-ring rotation in FoF1-ATP synthase. *EMBO J.* **28**, 2689−2696

75. Ishmukhametov, R., Hornung, T., Spetzler, D., and Frasch, W.D. (2010) Direct observation of stepped proteolipid ring rotation in E. coli F(o)F(1)-ATP synthase. *EMBO J.* **29**, 3911−3923